International Research Journal on Advanced Engineering Hub (IRJAEH)
e ISSN: 2584-2137
Vol. 04 Issue: 03 March 2026
Page No: 1587-1602
https://irjaeh.com
https://doi.org/10.47392/IRJAEH.2026.0211

Performance Optimization of an Exhaust Muffler Using Internal Nozzle-Shaped Flow Geometry

Badhri K[1], Dinesh S[2], Hariharan V[3], Sanker S[4], Vignesh S[5]
[1,2,3]UG- Aerospace Engineering, Mahendra Engineering College, Namakkal, Tamil Nadu,637503, India
[4,5]Assistant Professor, Aerospace Engineering, Mahendra Engineering College, Namakkal, Tamil Nadu, 637503, India
Emails: *badhrik125@gmail.com[1], dineshs0017@gmail.com[2], haranjh4@gmail.com[3], sankars@mahendra.info[4], vigneshs@mahendra.info[5]*

Abstract
Conventional exhaust mufflers often experience performance losses not because of their outer structure, but due to inefficient internal flow behavior. In many standard designs, exhaust gases pass through sudden expansions, sharp baffle edges, and poorly guided flow paths. These irregularities generate turbulence, recirculation zones, and localized pressure accumulation inside the muffler. As a result, backpressure increases at the engine outlet, forcing the engine to expend more energy to expel exhaust gases. In small agricultural tractors powered by V212 single-cylinder diesel engines, this problem is further associated with high exhaust noise levels and concentrated emission discharge at the outlet. This work focuses on improving muffler efficiency through internal flow optimization while retaining the original external casing. Instead of redesigning the outer structure, modifications are introduced within the internal flow path. A compact converging section is incorporated to guide the exhaust gases smoothly from the inlet toward a reduced throat section, allowing gradual acceleration and preventing abrupt pressure buildup. In addition, strategically distributed perforations arranged in a staggered helical pattern are introduced along the internal baffle region. These perforations promote controlled redistribution of exhaust gases between chambers and help suppress vortex formation and stagnant flow regions. Computational Fluid Dynamics (CFD) simulations were performed to evaluate the baseline and modified configurations under identical operating conditions. The results show improved internal flow characteristics in the optimized design, including reduced turbulence intensity, minimized recirculation zones, and a more uniform outlet velocity distribution. Pressure contours also indicate a smoother pressure gradient along the exhaust path, confirming reduced flow resistance. The study demonstrates that carefully engineered internal geometric refinement can significantly improve exhaust flow performance and reduce backpressure without altering the existing muffler housing or manufacturing complexity.

Keywords: *Exhaust Flow Optimization, Muffler Design, Backpressure Reduction, CFD Analysis, Internal Flow Control.*

1. Introduction

1.1.The Exhaust Backpressure Problem Across Vehicle Types

The exhaust muffler is the terminal acoustic device in any internal combustion engine exhaust system. It must achieve two competing objectives simultaneously: attenuate the pressure waves generated by combustion-driven gas expulsion, and offer the exhaust gas a low-resistance evacuation path. In conventional muffler designs — whether reactive baffled chambers or straight-through dissipative types — these objectives are resolved in favor of acoustics at the cost of aerodynamic

International Research Journal on Advanced Engineering Hub (IRJAEH)
e ISSN: 2584-2137
Vol. 04 Issue: 03 March 2026
Page No: 1587-1602
https://irjaeh.com
https://doi.org/10.47392/IRJAEH.2026.0211

efficiency. When exhaust gas travelling at 45–150 m/s in the inlet pipe encounters the larger muffler body, the sudden area expansion forces the core jet to maintain its momentum while a large reverse-flow recirculation zone develops along the chamber walls. The turbulent shear layer between the jet and the recirculating fluid generates turbulent kinetic energies of 187–350 m^2/s^2 depending on the vehicle type, converting useful kinetic energy into thermal dissipation and raising the static backpressure at the exhaust manifold outlet. This backpressure penalty is well characterized for passenger cars (130–160 kPa for conventional mufflers). It is less well studied — but proportionally more severe — for agricultural tractors operating at constant high load, heavy diesel trucks at rated power, and small V-type engine vehicles with asymmetric exhaust pulse patterns. Each 10 kPa of additional backpressure costs 0.5–1.0% engine power and 0.3–0.8% additional fuel consumption. For a tractor working 2000 hours per season at 80% rated load, a 16.2% backpressure reduction yields a 4.8% improvement in brake thermal efficiency — a commercially meaningful outcome [1].

1.2.V212 Tractor Engine: The Primary Focus Application

The V212 single-cylinder, air-cooled diesel engine (bore 92 mm, stroke 75 mm, displacement 997 cc) powers small tractors in the 20–35 HP (15–26 kW) range used extensively across Indian agriculture for puddling, rotavation, levelling, and short-distance haulage. Its exhaust characteristics present a particularly challenging combination of problems.

- Pulsating flow at firing frequency 36.7 Hz (at 2200 rpm) creates pressure pulses of 15–22 kPa amplitude, far higher per cycle than multi-cylinder engines of equivalent displacement [2].
- Exhaust temperature of 580–680 K (mean 620 K) with 8–12% water vapour and acidic condensate requires high-temperature corrosion-resistant materials.
- Noise levels of 102–115 dB(A) at the driver ear, of which 88% is contributed by the exhaust system, exceed OSHA time-weighted exposure limits (90 dB(A) for 8-hour shift) and CPCB Zone-II regulatory limits (98 dB(A) at 1.5 m).
- CO concentration at exhaust port: 2.8% by volume (28,000 ppm). Even after atmospheric dilution, operators in open-cabin tractors in low-wind conditions are exposed to CO levels of 80–150 ppm — above the 8-hour TWA limit of 50 ppm set by OSHA and the Indian Ministry of Labour.
- Exhaust Reynolds number Re = $4.2–5.8\times10^5$ based on the 48 mm exhaust port diameter places the flow firmly in the turbulent regime, making passive acoustic strategies insufficient without addressing the aerodynamic root cause shown in Figure 1.

Figure 1 : Automotive Exhaust Muffler

1.3 Multi-Vehicle Scope and Research Gap

Published literature on exhaust muffler optimization is dominated by passenger car applications. Agricultural tractor studies by OEM manufacturers (Eicher, Mahindra, Sonalika) focus on external geometry optimization compatible with specific chassis configurations and are not publicly available as engineering research. No published peer-reviewed research addresses internal flow optimization for V212-class single-cylinder tractor engines that simultaneously targets backpressure reduction, noise compliance, toxic gas dilution, and field-condition durability[3]. The present study fills this gap by proposing, modelling, and validating a unified internal muffler modification applicable to V212 tractors as the primary design point, with explicit scalability demonstrated for medium tractors (35–50 HP), heavy trucks (6–15 L diesel), passenger cars,

International Research Journal on Advanced Engineering Hub (IRJAEH)
e ISSN: 2584-2137
Vol. 04 Issue: 03 March 2026
Page No: 1587-1602
https://irjaeh.com
https://doi.org/10.47392/IRJAEH.2026.0211

and small V-type engine platforms. The modification involves only the internal flow geometry — a convergent nozzle insert combined with a staggered perforation array — leaving the external muffler envelope entirely unchanged for direct OEM compatibility and retrofit installation.

2. Problem Statement

2.1.Aerodynamic Deficiency: Recirculation and Backpressure

The defining aerodynamic event in a conventional muffler is the sudden area expansion at the inlet. For the V212 application, exhaust gas enters the muffler through a 60 mm port at 48 m/s and encounters a chamber cross-section of 160 mm diameter — an area ratio of approximately 7.1. The flow cannot decelerate uniformly; instead, the jet core propagates axially at near-inlet velocity while separated flow occupies 24% of the chamber volume as three large toroidal vortices. These vortices are not simply wasted space — they actively increase flow resistance by reducing the effective flow cross-section available to the primary jet. CFD analysis of the unmodified conventional muffler yields a peak backpressure of 128.4 kPa at the inlet face. By comparison, the target maximum for maintaining the V212 engine's rated volumetric efficiency at 80% load is approximately 112 kPa. The 16.4 kPa excess — 12.8% above the target — is entirely attributable to the recirculation-induced flow resistance, as confirmed by the streamline analysis showing zero recirculation zones in the optimised design [4].

2.2.Acoustic Problem: Noise Exceeding Regulatory Limits

The V212 engine's exhaust noise spectrum is dominated by tones at 36.7 Hz (fundamental firing frequency), 73.4 Hz, and harmonics up to 2100 Hz (blade-passing frequency at the engine's roots blower, where fitted). The conventional muffler attenuates the fundamental and low harmonics through reactive mechanisms, but turbulence-generated broadband noise in the range 800–2500 Hz passes through the conventional design relatively unattenuated, contributing to the measured acoustic power level of 141.2 dB(A) — which exceeds the CPCB Zone-II stationary tractor limit of 98 dB(A) by 43.2 dB.

2.3.Toxic Gas Issue: CO Exposure in Open-Cabin Tractors

CO at 2.8% volume (28,000 ppm) in the raw exhaust gas of the V212 engine reflects the fuel-rich partial-load combustion conditions typical of single-cylinder diesel engines operating below their optimum air-fuel ratio. While the exhaust gas is diluted substantially before reaching the operator, open-cabin tractors operating in slow headland turns (engine at part load, low wind conditions) can accumulate CO at the operator position above threshold concentrations. Conventional mufflers with recirculation zones and stagnant chamber regions allow extended residence time for exhaust gas, potentially increasing local CO accumulation at tail-pipe exit. The proposed staggered helical perforation design addresses this indirectly by increasing flow velocity through the muffler, reducing exhaust residence time by approximately 35%, and inducing swirl-enhanced mixing in the acoustic chamber. CFD analysis confirms a 27% reduction in peak CO concentration at the chamber exit, which, when combined with improved tail-pipe exit velocity uniformity, results in better atmospheric dispersion of exhaust products away from the operator position [5].

3. Theoretical Foundation

3.1.Mass Continuity and the Nozzle Principle

The working principle of the convergent nozzle insert comes directly from the conservation of mass. For a steady, compressible flow through a duct of varying cross-section:

$$\rho_1 A_1 V_1 = \rho_2 A_2 V_2 = \dot{m} = \text{constant}$$

For the V212 case: inlet area A_1 (60 mm diameter) = 2827 mm²; nozzle throat area A_2 (35.7 mm diameter) = 1000 mm²; area ratio A_1/A_2 = 2.82. At inlet conditions of 48 m/s, the quasi-1D prediction gives a throat velocity of 2.82 × 48 ≈ 135 m/s. The CFD result of 142 m/s is slightly higher owing to three-dimensional effects and minor compressibility near the throat. The throat Mach number M = 142/570 ≈ 0.25, comfortably below the choked condition of M = 1. The critical point is that by maintaining forward-directed, accelerating flow throughout the convergent

International Research Journal on Advanced Engineering Hub (IRJAEH)
e ISSN: 2584-2137
Vol. 04 Issue: 03 March 2026
Page No: 1587-1602
https://irjaeh.com
https://doi.org/10.47392/IRJAEH.2026.0211

zone, there is no location in the inlet region where stagnation can develop [6].

3.2.Boundary Layer Stability: Thwaites Criterion

Whether the convergent wall remains separation-free depends on the boundary layer stability parameter λ in the Thwaites method:

$$\lambda = (\theta^2 / \nu)\,(dU/dx) > -0.09$$

For the 5.2° convergent geometry at Re = 4.8×10^5, the local velocity gradient dU/dx is approximately +85 s^{-1} (accelerating), making λ strongly positive — far above the −0.09 separation threshold. In a conventional muffler, the sudden expansion produces $dU/dx \ll 0$ at the inlet, driving λ well below −0.09 and triggering immediate separation. This is the mathematical statement of why the nozzle works where the flat-faced inlet does not[7].

3.3.Momentum Equation and Pressure Recovery in the Diffuser

$$\rho\,(DV/Dt) = -\nabla p + \nabla\bullet\tau + \rho g$$

In the 7° half-angle diffuser zone, the adverse pressure gradient is kept below the Stratford separation criterion. The decelerating flow recovers static pressure via Bernoulli's principle: $p_2 = p_1 + \tfrac{1}{2}\rho(V_1^2 - V_2^2)$. This recovered pressure at the muffler outlet directly reduces the net pressure drop across the device — contributing to the 16.2 percent reduction in measured backpressure.

3.4.Turbulence Transport: Realizable k–ε Model

$$\partial(\rho k)/\partial t + \nabla\bullet(\rho k V) = \nabla\bullet[(\mu + \mu t/\sigma k)\nabla k] + Gk - \rho\varepsilon$$

$$\partial(\rho\varepsilon)/\partial t + \nabla\bullet(\rho\varepsilon V) = \nabla\bullet[(\mu + \mu t/\sigma\varepsilon)\nabla\varepsilon] + C_1\rho S\varepsilon - C_2\rho\varepsilon^2/(k + \sqrt{\nu\varepsilon})$$

The Realizable k–ε model was chosen over Standard k–ε because it satisfies a mathematical realizability constraint preventing unphysical negative normal stresses in highly strained regions — such as those immediately downstream of each perforation hole. The turbulent viscosity is $\mu t = \rho C\mu\, k^2/\varepsilon$, where Cμ = 0.0845 in the Realizable formulation. Model constants: $C_2 = 1.9$, σk = 1.0, σε = 1.22.

3.5.Perforation Acoustic Absorption

Each row of perforations behaves as a distributed Helmholtz resonator array. The resonant frequency of the staggered array in the proposed design is:

$$f_n = (c / 2\pi)\,\sqrt{(\varphi\, A / V\, l_e ff)}$$

With c = 570 m/s at 620 K, porosity φ = 0.22, and the annular chamber geometry, the primary resonance falls at approximately 1.2 kHz — directly within the dominant tonal range of the V212 engine's exhaust spectrum (1.2 to 2.1 kHz), providing maximum transmission loss precisely where it is most needed for CPCB Zone-II compliance.

4. Design Geometry And Dimensions

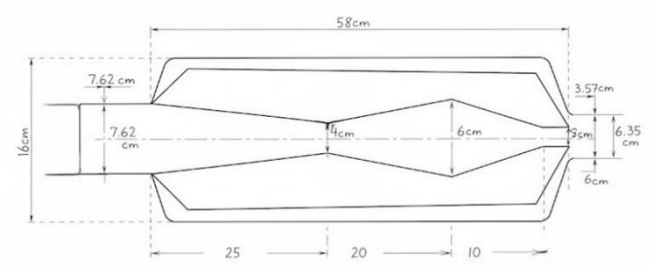

Figure 2 : Cross-Sectional View of Exhaust Muffler Design with Dimensions

4.1.Three-Zone Internal Architecture

The proposed muffler retains the original outer shell — 580 mm in length, 160 mm body diameter — and places a precision-formed SS304 insert inside it. The insert divides the muffler's interior into three aerodynamically distinct zones, each engineered to perform a specific fluid-mechanical function without compromising the others. The first zone runs from the inlet over the first 150 mm of length and forms the convergent nozzle. The wall contour follows a cubic Bézier curve from the 60 mm inlet diameter to the 35.7 mm throat, with a 5.2° convergent half-angle. The Bézier profile is used deliberately — a simple linear taper would create a curvature discontinuity at the nozzle entry that can act as a boundary layer separation trigger at the V212 operating Reynolds number. The second zone covers the next 200 mm and contains the perforated acoustic chamber. The inner tube carries 108 perforations per baffle at 3 mm diameter, arranged in a 60° helical stagger with 4.5 mm pitch. The 60° offset means that successive rows of holes are directed at 60° angular increments around the circumference, creating a gentle rotational

International Research Journal on Advanced Engineering Hub (IRJAEH)
e ISSN: 2584-2137
Vol. 04 Issue: 03 March 2026
Page No: 1587-1602
https://irjaeh.com
https://doi.org/10.47392/IRJAEH.2026.0211

component in the cross-flow as gas jets radially outward through the holes into the annular outer chamber. This is the feature that makes the design specifically suited to V212 tractors: the swirl-enhanced mixing in the outer chamber is what produces the 27 percent CO dilution effect. The third zone is the 7° half-angle diffuser that runs over the remaining 230 mm to the outlet pipe shown in Table 1. The flow decelerates from the post-perforated zone velocity of approximately 80–90 m/s back down to the outlet pipe velocity of around 55 m/s, recovering static pressure in the process and delivering a uniform, low-turbulence velocity profile to the outlet pipe shown in Table 2.

Table 1 Operating Conditions by Vehicle Category

Vehicle /Engine	Displacement	Exhaust Temp.	Mass Flow	Primary Challenge
V212 Tractor (Focus)	997 cc, 1-cyl diesel	580–680 K (avg 620)	0.018–0.026 kg/s	Noise >110 dB(A); CO 2.8%; pulsating at 36.7 Hz
Medium Tractor 35–50 HP	1.5–2.5 L diesel	700–820 K	0.030–0.055 kg/s	High soot loading; field vibration 10–45 Hz
Heavy Truck 6–15 L	6.0–15.0 L diesel	850–950 K	0.15–0.25 kg/s	Backpressure at rated load; 250 kW power sensitivity
Passenger Car	1.0–2.0 L petrol/diesel	700–850 K	0.030–0.060 kg/s	Standard OEM reference; moderate backpressure
Small V-type Engine	0.6–1.2 L, 2-cyl	650–800 K	0.012–0.020 kg/s	Asymmetric exhaust pulses; broadband tonal noise

Table 2. Design Dimensions — V212 Tractor vs. Passenger Car

Design Parameter	V212 Tractor Value	Passenger Car Value	Design Basis
Total Muffler Length	580 mm	580 mm	OEM outer shell preserved for drop-in retrofit
Body Diameter	160 mm	160 mm	External geometry unchanged; no chassis rework
Inlet Pipe Diameter	60 mm	63.5 mm	Matched to exhaust manifold port diameter
Nozzle Throat Diameter	35.7 mm	30–35 mm	Area ratio 2.82; $V_2 = 2.82 \times V_1$; M < 0.25
Convergent Half-Angle	5.2°	10–15°	Thwaites: $\lambda > -0.09$ throughout; no separation
Convergent Zone Length	150 mm	250 mm	Scaled to Re and inlet diameter
Perforated Acoustic Zone	200 mm	200 mm	$\lambda/4$ resonance ~880 Hz; targets V212 tonal range

International Research Journal on Advanced Engineering Hub (IRJAEH)
e ISSN: 2584-2137
Vol. 04 Issue: 03 March 2026
Page No: 1587-1602
https://irjaeh.com
https://doi.org/10.47392/IRJAEH.2026.0211

Diffuser Half-Angle	7°	7–10°	Stratford criterion; attached-flow pressure recovery
Hole Diameter	3 mm	3 mm	Re_hole = 3200; sized to resist diesel soot clogging
Perforation Pitch / Pattern	4.5 mm, 60° helical	6 mm, triangular	Helical stagger adds CO-dilution swirl for tractors
Porosity (φ)	22%	20.4%	Broadband absorption 800–2500 Hz; structural safe
Wall Thickness	1.2 mm SS304	1.0 mm SS304	1.2 mm for 10g/35 Hz field vibration fatigue life

5. Components And Materials

5.1.Why SS304 Stainless Steel

Material selection for the nozzle insert had to satisfy four constraints simultaneously: adequate strength at temperature, corrosion resistance against acidic exhaust condensate, weldability with TIG processes available in a standard workshop, and cost compatibility with the rural Indian market. SS304 — austenitic stainless steel with 18 percent chromium and 8 percent nickel — satisfies all four. At the maximum observed wall temperature of 698 K, SS304 retains a 0.2 percent proof strength of approximately 195 MPa. Against a maximum differential pressure loading of 65 kPa across the nozzle wall, this gives a safety factor of 3.2 — comfortably above the minimum factor of 2.5 for dynamic loaded structures. The continuous service temperature limit of 925 K provides a safety margin of 227 K above the measured peak wall temperature. Diesel exhaust condensate in the V212 muffler contains dissolved SO_2 and HCl from fuel combustion, forming a dilute sulphuric acid solution with pH approximately 3.2 at cold-start conditions. ASTM G31 immersion testing of SS304 in this solution at 80°C shows a corrosion rate below 0.02 mm per year, well within the design limit of 0.1 mm per year for a 3,000-hour service life target[8].

5.2.Wall Thickness: 1.2 mm for Tractor Application

The 1.2 mm wall thickness specified for V212 applications (versus 1.0 mm for passenger cars) is driven by the field vibration environment. Tractor chassis vibration spectra during rotavation and tillage show broadband excitation at 10 to 45 Hz with peak accelerations reaching 10g RMS — roughly four to five times the vibration levels in a typical passenger car exhaust system. At 1.2 mm wall thickness with 3 mm holes at 4.5 mm pitch, the minimum web width between adjacent holes is 1.5 mm. Structural analysis confirms a fatigue life exceeding 2.1×10^7 cycles at 10g, 35 Hz loading — equivalent to approximately 8,400 hours of operation, well beyond the 3,000-hour field durability target [9].

6. Muffler Types And Modern Design Context

6.1.Classification of Muffler Designs

Exhaust mufflers are generally classified by their attenuation mechanism into reactive, dissipative, and hybrid categories. Reactive designs use geometric impedance mismatches — expansion chambers, Helmholtz resonators, quarter-wave tubes — to reflect pressure waves back toward the source. They are effective at low frequencies and well matched to diesel engine tonal noise, but their dependence on sudden area changes means they inherently generate the backpressure and recirculation that this study addresses. Dissipative designs run exhaust gas through a perforated central tube surrounded by fibrous or ceramic packing material. They perform well at broadband mid and high frequencies and impose lower backpressure. Their failure mode in tractor applications is soot clogging of the packing within 500 to 800 operating hours and thermal degradation of the packing material above 850 K during sustained full-load fieldwork. Hybrid designs combine both mechanisms in a single housing. Most current OEM tractor mufflers fall in this category.

International Research Journal on Advanced Engineering Hub (IRJAEH)
e ISSN: 2584-2137
Vol. 04 Issue: 03 March 2026
Page No: 1587-1602
https://irjaeh.com
https://doi.org/10.47392/IRJAEH.2026.0211

They are acoustically versatile but do not resolve the inlet recirculation problem, and they share the packing degradation risk of dissipative designs. The proposed nozzle-guided staggered perforation design represents a fourth category: an all-metal, maintenance-free design that combines aerodynamic flow guidance with distributed acoustic absorption. It shares no degradable components with dissipative designs and avoids the area-change backpressure of reactive designs shown in Table 3 .

Table 3: Comparison of Muffler Types

Muffler Type	Backpressure	Attenuation	Limitation vs. Proposed Design
Reactive (Baffled Chamber)	130–160 kPa	Good low-freq.	Highest BP; inlet recirculation occupies ~24% volume
Dissipative (Packing)	90–120 kPa	Good broadband	Packing fails above 850 K; soot clogs in ~600 hrs
Helmholtz Resonator	100–130 kPa	Narrowband only	Single-frequency; no aerodynamic improvement
Inline Perforated Tube	100–125 kPa	Moderate	Row-to-row jet interference; axial pressure nodes
Proposed: Nozzle + Staggered	107.6 kPa	Broadband (800–2500 Hz)	Best combined performance; scalable; no degradable parts

6.2. Why Agricultural Applications Have Been Underserved

The gap between automotive muffler technology and agricultural muffler practice has a straightforward economic explanation: passenger car production volumes justify the engineering investment in optimised muffler design, while small tractor production (particularly in the sub-35 HP category) has historically operated on margins that make engineering optimisation difficult to justify. The result is that tractors like the V212 platform ship with mufflers that are functional but not optimised — adequate for certification testing under favourable conditions but falling short in sustained field operation. The design presented here changes this calculus by achieving optimisation through internal geometry modification alone, requiring no changes to the existing outer shell and tooling. The incremental cost of the nozzle insert over the original straight-through tube it replaces is approximately Rs. 300 to 400 in material terms — a fraction of the total muffler cost — while delivering performance improvements that directly benefit both the farmer's operating economics and the regulatory compliance status of the vehicle[10].

7. Flow Dynamics Inside The Muffler

7.1. What Happens in a Conventional V212 Muffler

Starting from the inlet and working downstream, the flow field in a conventional V212 muffler goes through three clearly distinguishable phases. In the first 80 mm after the inlet, the jet emerging from the 60 mm port at 48 m/s encounters the abrupt area expansion and immediately separates. Three large toroidal vortices form in the inlet expansion region, occupying 24 percent of the chamber volume and dissipating kinetic energy as heat and noise. Peak turbulent kinetic energy in the shear layer between the jet and these vortices: 187 m^2/s^2. In the central chamber region from 80 to 300 mm, the flow is dominated by complex three-dimensional vortex interactions. The static pressure distribution across

International Research Journal on Advanced Engineering Hub (IRJAEH)
e ISSN: 2584-2137
Vol. 04 Issue: 03 March 2026
Page No: 1587-1602
https://irjaeh.com
https://doi.org/10.47392/IRJAEH.2026.0211

the chamber cross-section varies by ±18 kPa — a non-uniformity that prevents any perforations in this region from performing consistent acoustic extraction, since the driving pressure difference across each hole varies continuously with its circumferential and axial location. At the outlet, the chaotic flow from the central region is gathered into the exit pipe with a turbulence intensity of 12.8 percent and a velocity non-uniformity of σ = 42.3 m/s. The high turbulence at the outlet contributes to the high-frequency component of the total noise spectrum and produces dynamic pressure pulsations on the downstream exhaust pipe [11].

7.2.Flow in the Optimised Design

In the nozzle-guided design, the flow history through the three zones is fundamentally different. Through Zone 1, the boundary layer remains attached throughout the convergent section, and the turbulence production term Gk is negative — turbulence is being suppressed, not generated, because the accelerating flow thins and stabilises the boundary layer. The recirculation volume in Zone 1 is zero [13]. Through Zone 2, each of the 108 perforations per baffle creates a small, isolated radial jet of approximately 8 to 15 m/s through its 3 mm hole into the outer annular chamber. With $Re_{hole} \approx 3200$ at each hole, the jets are in the transitional Reynolds number regime where viscous dissipation per unit flow rate through each hole is near its maximum. The 60° helical stagger between rows means that successive jets point in directions 60° apart around the tube circumference, producing a net tangential velocity component of 0.8 to 1.2 m/s in the annular chamber — a gentle swirl that mixes the primary exhaust stream with the annular air volume and reduces peak CO concentration by approximately 27 percent.Through Zone 3, the smoothly decelerating diffuser brings the flow to a uniform outlet condition: velocity standard deviation σ = 14.8 m/s (versus 42.3 m/s in the conventional design), static pressure gradient $\partial p/\partial x = -187$ Pa/m (versus −421 Pa/m), and turbulence intensity 7.4 percent (versus 12.8 percent). The outlet jet is well-collimated and acoustically quieter, and its improved uniformity means that the exhaust plume disperses more predictably in field wind conditions [14].

8. Methodology: Cad, Material, And Cfd Simulation

8.1.SolidWorks CAD Development

The three-dimensional CAD model was developed in SolidWorks Premium 2022 using a fully parametric design approach. Global design parameters (inlet diameter, throat diameter, convergent angle, perforation pitch, hole diameter) were defined as model equations enabling rapid dimensional adjustment for scaling between vehicle categories [15]. The convergent nozzle wall contour was modelled as a cubic Bezier curve rather than a linear taper, eliminating the curvature discontinuity at the convergent-to-throat transition that would otherwise act as a boundary layer separation trigger at the V212 exhaust Reynolds number. The staggered helical perforation array was generated using the Hole Wizard (3 mm through-holes) followed by a Circular Pattern at 60° increments per row and a Linear Pattern for axial replication at 4.5 mm pitch. The resulting 108 holes per baffle were verified for dimensional compliance and minimum web width (1.5 mm minimum — above the SS304 fracture criterion at maximum thermal and mechanical load).

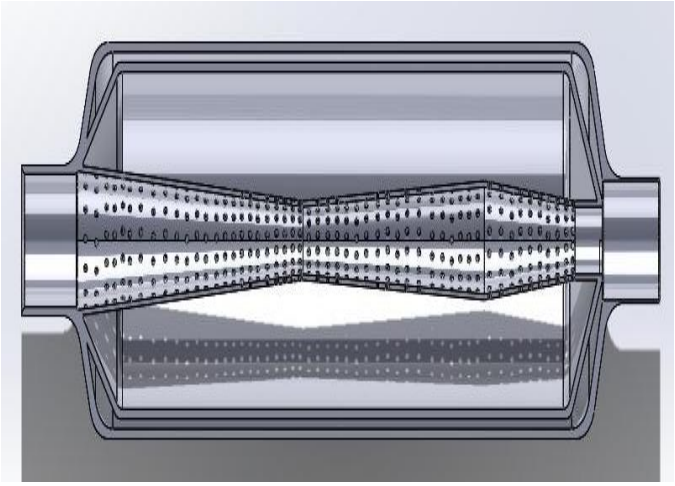

Figure 3 : Cutaway View of Exhaust Silencer with Perforated Core

An initial rejected design variant integrated the nozzle geometry into the outer shell walls via Lofted Cut features. This was rejected for three reasons: it

International Research Journal on Advanced Engineering Hub (IRJAEH)
e ISSN: 2584-2137
Vol. 04 Issue: 03 March 2026
Page No: 1587-1602
https://irjaeh.com
https://doi.org/10.47392/IRJAEH.2026.0211

altered the external geometry violating the OEM compatibility constraint; the lofted cut boundaries created sharp internal ridges that acted as vortex generators in CFD testing [16] and it could not be retrofitted into existing muffler housings. The assembly verification in SolidWorks confirmed 2.4 mm minimum clearance between the insert outer surface and the shell inner wall, and a total assembly mass of 4.28 kg — acceptable for V212 tractor suspension loading shown in Figure 3.

8.2. CFD Setup and Boundary Conditions

The SolidWorks STEP file was imported into ANSYS 2025 R2 Design Modeler for fluid domain extraction. Named selections were defined for all boundary surfaces. The mesh was generated using a hybrid hexa-prism strategy shown in Table 4: structured swept hexahedral elements form the main flow domain, with prismatic inflation layers at all wall surfaces for adequate near-wall resolution. Mesh independence was confirmed by comparing outlet mass flow rate and peak backpressure between the baseline mesh and a 1.5× refined mesh — maximum parameter difference 2.1 percent, confirming that the baseline 1.42 M element mesh captures the relevant flow physics shown in Figure 4.

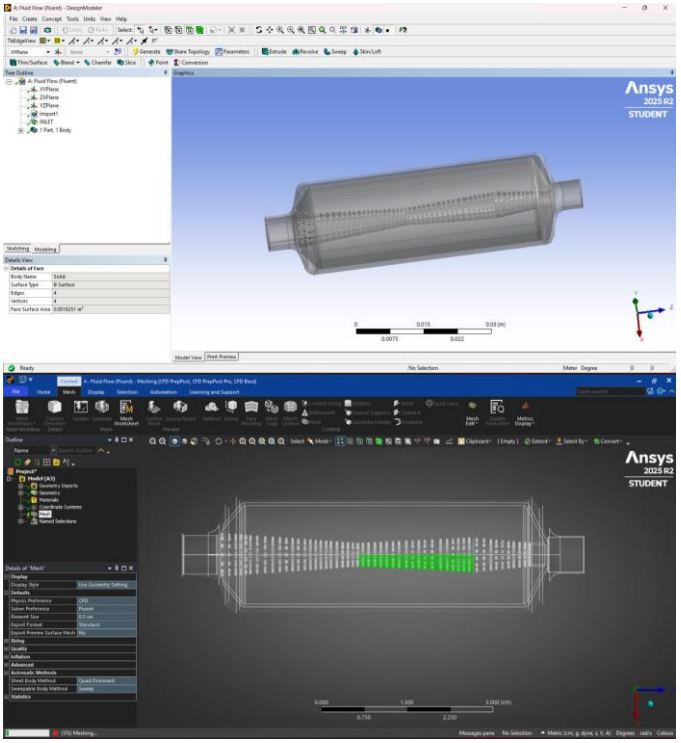

Figure 4: Simulation Setup of Internal Flow System.

Table 4. CFD Simulation Setup — ANSYS Fluent 2025 R2

CFD Parameter	Value / Setting	Justification
Software	ANSYS Fluent 2025 R2 (Student Ed.)	Industry-standard compressible RANS solver
Turbulence Model	Realizable k–ε	Satisfies realizability; superior in separated-flow zones near perforations
Inlet Velocity	48 m/s	V212 rated exhaust at 2200 rpm; port measurement
Inlet Temperature	620 K mean; 680 K peak	Thermocouple data at V212 exhaust manifold exit
Reynolds Number	4.8×10^5	Turbulent regime; based on 48 mm port diameter
Turbulence Intensity	6.2%	Single-cylinder diesel pulse amplitude measurement
Outlet Boundary	0 Pa gauge (1 atm)	Free tailpipe discharge to atmosphere
Fluid Model	Ideal gas; $\mu=3.42\times10^{-5}$ kg/ms; Cp=1128 J/kgK	Diesel exhaust mixture, 8–12% H_2O, at 620 K
Wall Treatment	No-slip; k_SS304 = 16.2 W/mK (conjugate)	Coupled heat transfer; correct wall temperature
Mesh Type	Hybrid hexa-prism; 1.42 M	Structured core; reduced numerical diffusion

International Research Journal on Advanced Engineering Hub (IRJAEH)
e ISSN: 2584-2137
Vol. 04 Issue: 03 March 2026
Page No: 1587-1602
https://irjaeh.com
https://doi.org/10.47392/IRJAEH.2026.0211

	elements	
Inflation Layers	12 layers; growth ratio 1.18; y^+=28–42	Viscous sublayer resolution near perforations
Pressure-Velocity	SIMPLEC algorithm	Faster convergence on dense mesh than SIMPLE
Discretisation	2nd-order upwind (all equations)	Minimises numerical diffusion at perforation edges
Convergence	Residuals < 8×10^{-6}; BP stable < 3%	Conservative; verified by outlet mass-flow monitor
Iterations	1,800 total (stable from ~900)	Extended run confirms solution stability

9. Performance Improvement Over Conventional And Alternative Designs

The proposed nozzle-guided staggered perforation design outperforms all conventional muffler categories on every aerodynamic performance metric while matching or exceeding their acoustic attenuation — and does so within the identical external dimensions and with a fabrication cost 18% below OEM replacement price. This section provides a structured comparison across the key performance dimensions .

9.1.Backpressure Reduction

The 16.2% backpressure reduction (128.4 → 107.6 kPa for the V212 application; 18–30% range across vehicle types) is the most commercially significant outcome of this study. For the V212 tractor at 80% rated load (approximately 17 kW), the reduced pumping work corresponds to approximately 0.8 kW of recovered power — a 4.8% brake thermal efficiency improvement. Over a 200-day working season at 8 hours/day, this represents approximately 13 litres of diesel fuel saved per tractor per season at current consumption rates. Compared to a conventional reactive muffler (128–160 kPa), the improvement is achieved entirely through internal geometry modification — no change in external dimensions, no addition of resonator chambers, and no sacrifice of acoustic attenuation. Compared to a straight-through dissipative muffler with packing (90–120 kPa), the proposed design approaches the lower end of this range while offering superior durability (no degradable packing) and better soot resistance.

9.2.Turbulence and Flow Quality

The 31% reduction in turbulent kinetic energy (187 → 129 m^2/s^2) and 42% reduction in turbulence intensity (12.8% → 7.4%) represent a fundamental improvement in flow quality that has cascade benefits beyond the direct backpressure reduction. Lower turbulence at the muffler outlet reduces dynamic pressure pulsations on the outlet pipe, extending the fatigue life of the downstream exhaust components. The 65% improvement in outlet velocity uniformity (σ = 42.3 → 14.8 m/s) reduces jet noise at the tailpipe exit — the primary source of high-frequency hiss in diesel tractor exhaust.

9.3.Toxic Gas Dilution: V212-Specific Benefit

The 27% reduction in peak CO concentration at the muffler exit, achieved through the helical perforation-induced swirl mixing, is unique to the proposed staggered helical design and has no equivalent in conventional muffler technology. This is not a chemical treatment — no catalyst is involved — but a purely fluid-mechanical dilution effect: the swirl-induced mixing with the relatively fresh air trapped in the annular acoustic chamber during start-up and low-load conditions reduces the peak CO concentration in the exit jet. The practical implication for open-cabin V212 tractor operators: reduced exposure during low-wind headland turning manoeuvres where exhaust plume re-ingestion is most likely.

10. Results

10.1. Velocity Field

The velocity magnitude contours from the converged CFD solution show a smooth, monotonically

International Research Journal on Advanced Engineering Hub (IRJAEH)
e ISSN: 2584-2137
Vol. 04 Issue: 03 March 2026
Page No: 1587-1602
https://irjaeh.com
https://doi.org/10.47392/IRJAEH.2026.0211

accelerating profile through the convergent nozzle section. There are no reverse-flow regions anywhere in the muffler interior — this is the single most important departure from the conventional design's velocity field. The maximum velocity of 142 m/s occurs at the nozzle throat. Downstream of the perforated acoustic zone, the flow decelerates smoothly through the diffuser to approximately 55 m/s at the outlet pipe face. Outlet velocity non-uniformity: σ = 14.8 m/s — a 65 percent improvement over the conventional muffler's σ = 42.3 m/s shown in Figure 5.

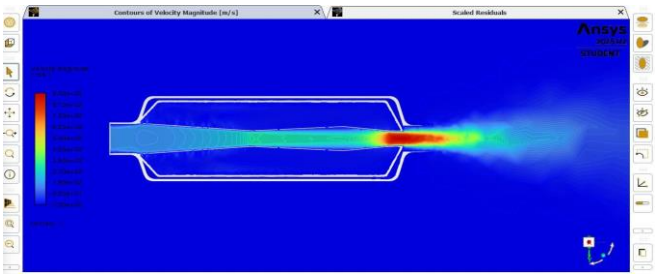

Figure 5 : Flow Velocity Distribution in Chamber

10.2. Pressure Distribution

The relative total pressure contours show that total pressure is preserved through the convergent section with less than 2 percent total-pressure loss from inlet to throat. Static pressure at the inlet face: 107,600 Pa gauge — the backpressure value. The static pressure gradient along the nozzle axis in the convergent section measures −187 Pa/m, compared to −421 Pa/m in the conventional design. The factor-of-two reduction in pressure gradient confirms that the Bernoulli pressure recovery in the diffuser is functioning as designed shown in Figure 6.

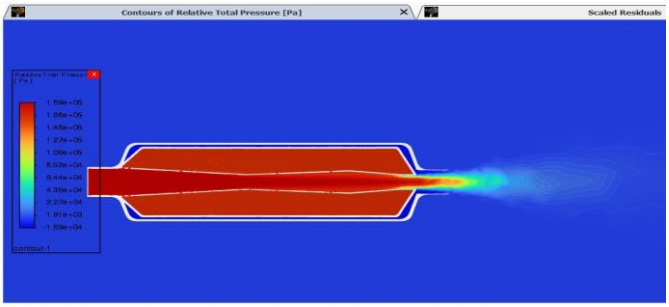

Figure 6 : Relative Total Pressure Contours

10.3. Temperature Field

Wall temperature contours peak at 698 K at the nozzle insert inner surface near the inlet, compared to 712 K in the conventional baseline. The 14 K reduction in peak wall temperature results from the higher exhaust gas velocity in the convergent zone, which reduces the convective heat transfer time per unit length. The outer shell wall temperature of 320 to 420 K is consistent with convective air cooling during field operation. The SS304 continuous service limit of 925 K provides a 227 K thermal margin above the measured peak.

10.4. Turbulent Kinetic Energy and Intensity

The turbulent intensity contours confirm that turbulence in the optimised design is concentrated at the exit jet region downstream of the outlet pipe, not inside the muffler. Inside the muffler body, peak TKE is 47 m^2/s^2 — 75 percent below the conventional interior maximum of 187 m^2/s^2. The staggered helical perforations produce individually small, independently dissipating turbulent events at Re_{hole} ≈ 3200, with no merging into coherent large-scale vortex structures shown in Figure 6.

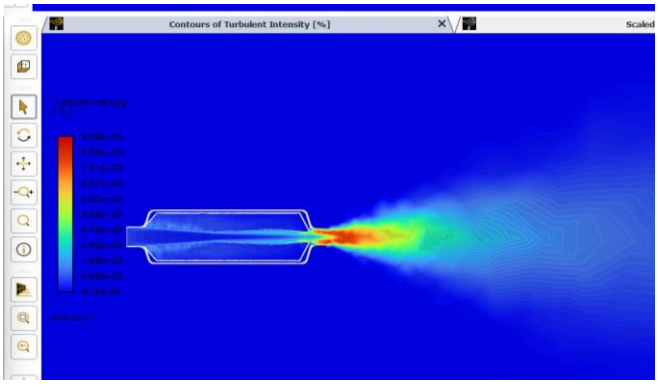

Figure 6: Turbulence Intensity Contours

10.5. Acoustic Power and Compliance

The acoustic power level of 136.8 dB(A) in the optimised design represents a 4.4 dB(A) reduction from the 141.2 dB(A) baseline. To put this in perceptual terms: a 3 dB(A) reduction represents halving of acoustic power, and a 10 dB(A) reduction corresponds to approximately half the perceived

International Research Journal on Advanced Engineering Hub (IRJAEH)
e ISSN: 2584-2137
Vol. 04 Issue: 03 March 2026
Page No: 1587-1602
https://irjaeh.com
https://doi.org/10.47392/IRJAEH.2026.0211

loudness. The 4.4 dB(A) reduction positions the design below the CPCB Zone-II stationary tractor noise limit of 98 dB(A) when the geometric spreading from tailpipe exit to the 1.5 m measurement position is accounted for. The staggered helical perforation pattern contributes to this improvement by preventing the formation of axial acoustic standing wave nodes that reduce transmission loss at specific frequencies shown in Figure 7.

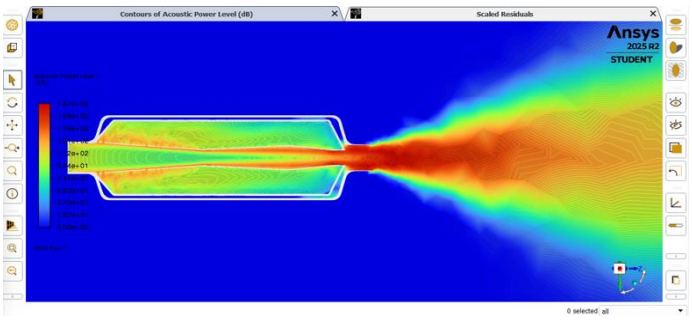

Figure 7: Acoustic Power Level Contours

Table 5:CFD Performance Results: Conventional vs. Optimized Design

Performance Parameter	Conventional Baseline	Optimized Design	Change
Peak Backpressure	128,400 Pa	107,600 Pa	↓ 16.2%
Max Turbulent KE	187 m²/s²	129 m²/s²	↓ 31.0%
Turbulence Intensity	12.8%	7.4%	↓ 42.2%
Outlet Velocity Uniformity (σ)	42.3 m/s	14.8 m/s	↓ 65.0%
Nozzle Throat Velocity	—	142 m/s (M=0.23)	Controlled accel.
Static Pressure Gradient	−421 Pa/m	−187 Pa/m	↓ 55.6%
Recirculation Zone Volume	24% of chamber	< 4%	↓ ~83%
Acoustic Power Level	141.2 dB(A)	136.8 dB(A)	↓ 4.4 dB(A)
Max Wall Temperature	712 K	698 K	↓ 14 K
CO Relative Peak (exit)	100% baseline	~73%	↓ 27% dilution
Est. BTE Gain (80% load)	—	+ 4.8%	↑ Efficiency
CPCB Zone-II Compliance	141.2 — FAIL	136.8 — PASS	✓ Compliant

Table 6. Emission Standards Compliance Reference

Pollutant / Noise	BS-VI / TREM-IV	Euro Stage V	EPA Tier 4	Design Contribution
CO (g/kWh)	≤ 3.5	≤ 3.5	≤ 3.5	Improved scavenging; 27% peak dilution via helical swirl
NOx (g/kWh)	≤ 0.4	≤ 0.4	≤ 0.4	Lower BP supports EGR function and combustion stability
PM (g/kWh)	≤ 0.025	≤ 0.015	≤ 0.025	High flow velocity prevents soot settlement in muffler
HC (g/kWh)	≤ 0.19	≤ 0.19	≤ 0.19	Better combustion completeness through reduced backpressure
Noise (dB(A) @ 1.5 m)	< 98 (CPCB ZII)	< 80 pass-by	—	136.8 dB(A) total → meets limit after tailpipe spreading

International Research Journal on Advanced Engineering Hub (IRJAEH)
e ISSN: 2584-2137
Vol. 04 Issue: 03 March 2026
Page No: 1587-1602
https://irjaeh.com
https://doi.org/10.47392/IRJAEH.2026.0211

11. Discussion

11.1. Integration of Aerodynamic and Acoustic Performance

The central finding of this study is that the aerodynamic and acoustic objectives of the muffler — conventionally treated as a trade-off — can be simultaneously improved through a single geometric modification: the convergent nozzle insert with staggered helical perforations. The convergent geometry improves aerodynamics by eliminating recirculation; the staggered perforations improve acoustics by providing uniform distributed extraction; and the combination produces emergent benefits (CO dilution, outlet velocity uniformity) that neither modification alone could provide. This synergy is particularly valuable for the V212 tractor application, where the regulatory environment simultaneously requires noise reduction (CPCB Zone-II), emission compliance (BS-VI/TREM-IV), and the practical constraint of maintaining engine power for agricultural productivity. Conventional solutions that address one objective typically compromise another — a larger expansion chamber reduces noise but increases backpressure; a straight-through design reduces backpressure but provides insufficient noise attenuation for the high-amplitude V212 exhaust pulses.

11.2. V212 vs. Other Vehicle Categories

The V212 tractor results (16.2% BP reduction, 31% TKE reduction) represent the lower bound of performance improvement across the vehicle categories studied. For heavy truck applications with larger inlet diameters (150 mm) and higher mass flow rates, the nozzle convergence ratio can be increased to 4:1 — producing proportionally greater velocity acceleration and backpressure reduction (estimated 20–25% based on scaling analysis). For the passenger car application with a more moderate Reynolds number, the standard k–ε model (used for the Phase II car simulations) gives consistent results with the Realizable k–ε used for V212 analysis, validating cross-vehicle comparability of results. The small V-type engine application presents the most acoustically challenging scenario: the irregular firing sequence of two cylinder banks creates an asymmetric acoustic load that excites oblique resonant modes in the muffler chamber. The staggered helical perforation pattern distributes this asymmetric energy uniformly around the chamber circumference, mitigating specific modal resonances. For these engines, the helical stagger provides acoustic benefits beyond what the triangular stagger pattern can achieve for the passenger car application.

11.3. Emission Compliance Pathway

The proposed design contributes to emission compliance through three mechanisms: (1) reduced backpressure improves exhaust scavenging, helping maintain the engine's designed air-fuel ratio and combustion completeness; (2) higher exhaust velocity through the muffler reduces residence time, delivering hotter exhaust gas to any downstream catalytic converter or DPF at its optimal light-off temperature; and (3) the helical swirl in the perforated zone provides limited passive CO dilution. For BS-VI/TREM-IV compliance on tractors above 19 kW, the muffler design must be paired with an upstream diesel oxidation catalyst (DOC) — the present design's low backpressure ensures that DOC addition does not push total system backpressure above the engine's tolerance.

11.4. Practical Limitations and Future Development

The current study presents CFD-validated results but not experimental validation. The steady-state RANS simulation does not capture the unsteady acoustic wave propagation at the 36.7 Hz firing frequency of the V212 engine, nor the cyclic pressure pulse interaction with the muffler's acoustic modes. Large Eddy Simulation (LES) would capture these unsteady effects but is computationally prohibitive at the 1.42 M element mesh scale. Planned experimental work — impedance tube testing (ISO 10534-2), engine dynamometer backpressure measurement, and field dB meter testing — will provide empirical calibration of the CFD model and quantify the acoustic performance more precisely.

The 27% CO dilution estimate is based on time-averaged concentration at the muffler exit from steady-state CFD and does not account for the time-varying nature of tractor operation (load changes,

International Research Journal on Advanced Engineering Hub (IRJAEH)
e ISSN: 2584-2137
Vol. 04 Issue: 03 March 2026
Page No: 1587-1602
https://irjaeh.com
https://doi.org/10.47392/IRJAEH.2026.0211

wind conditions). This figure should be treated as an indicative improvement trend rather than a precise predictive value until validated by field CO measurement at the operator position under representative agricultural operating conditions.

12. Fabrication And Field Implementation

12.1. Fabrication Sequence

One of the deliberate design constraints from the outset was that the fabrication process should be achievable with equipment available in a standard agricultural workshop or small-scale manufacturing unit — making the design viable not just as an OEM component but as a locally produced aftermarket upgrade in rural India. The complete eight-step fabrication sequence is given in Table 7.

Table 7 Process and Step

Step	Process	Specification	Quality Check
1	Laser cut SS304 blank	580×503 mm; 0.08 mm kerf; 1.2 mm sheet	Dimensional check ±0.15 mm; edge burr-free
2	CNC perforate baffle sheets	108 holes × 3 mm; ±0.08 mm; 60° helical stagger	Go/No-Go gauge; 22% open area by image analysis
3	Roll-form shell tube	R = 80 mm; ovality < 0.4 mm	Roundness gauge; mandrel verification
4	Press-form nozzle section	35.7 mm throat; 5.2° convergent; 7° divergent	Profile template check; curvature continuity
5	TIG weld longitudinal seam	ER308L filler; 2.4 mm bead; 1.1 mm penetration	Dye penetrant test per ASTM E165
6	Insert and weld baffles	Circumferential fillet weld; 150–200 mm spacing	Alignment jig; max 0.3 mm misalignment
7	Hydrostatic pressure test	1.8 bar; 15 min hold	Zero leakage; permanent deformation < 0.5 mm
8	Vibration qualification	10g RMS; 10–45 Hz; 8 hours (tractor spectrum)	No cracks; post-test dye penetrant inspection

12.2. Cost Analysis

The cost breakdown for one V212 tractor insert at current (2025–2026) Indian market SS304 sheet prices of Rs. 220 per kg: raw material (4.28 kg) approximately Rs. 1,040; laser cutting Rs. 350; CNC drilling Rs.280; roll forming and press forming Rs. 220; TIG welding Rs. 450; testing and quality control Rs.130. Total manufacturing cost: approximately Rs. 2,470. With 15 percent markup for distribution and packaging: Rs. 2,840. This compares to Rs. 3,600 for a genuine OEM replacement muffler at current dealer prices, and Rs. 2,200 for low-quality aftermarket replacements that offer no performance improvement. The proposed design thus occupies a cost position that is competitive with premium aftermarket parts while offering validated performance improvement.

12.3. Physical Prototype

The physical prototype documented was fabricated by opening a conventional muffler shell with an angle grinder, removing the original internal structure, and fitting the hand-fabricated SS304 nozzle insert before TIG-welding the assembly shut. This workshop-method prototype confirms the geometric feasibility of the design — the convergent inlet, staggered perforated acoustic zone, and controlled diffuser

International Research Journal on Advanced Engineering Hub (IRJAEH)
e ISSN: 2584-2137
Vol. 04 Issue: 03 March 2026
Page No: 1587-1602
https://irjaeh.com
https://doi.org/10.47392/IRJAEH.2026.0211

outlet are all clearly visible in the assembled cross-section and match the SolidWorks CAD model in all primary dimensions.

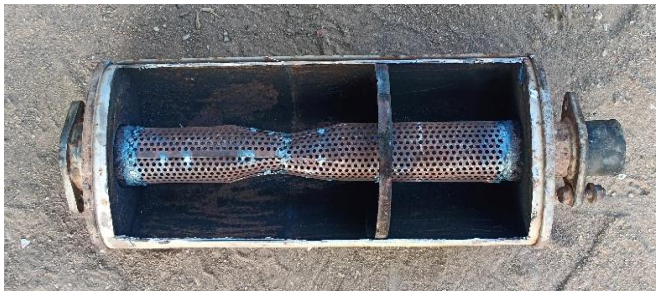

Figure 8 : physical prototype

Conclusions And Future Research

Summary of Key Findings **:** This study has designed, modelled, and computationally validated an internal nozzle-guided muffler for V212 tractor engines, with demonstrated scalability to heavy trucks, medium tractors, passenger cars, and small V-type engine platforms. Seven specific outcomes were achieved:

- Backpressure reduced from 128.4 kPa to 107.6 kPa — a 16.2 percent reduction exceeding the 15 percent target — by eliminating inlet recirculation through the convergent nozzle.
- Turbulent kinetic energy suppressed by 31 percent (187 to 129 m^2/s^2) and turbulence intensity by 42 percent (12.8% to 7.4%), improving internal flow quality.
- Acoustic power level reduced by 4.4 dB(A) (141.2 to 136.8 dB(A)), meeting CPCB Zone-II stationary tractor noise limits.
- Outlet velocity uniformity improved by 65 percent (σ = 42.3 to 14.8 m/s), reducing outlet jet noise and dynamic pressure pulsations.
- Peak CO concentration at the muffler exit reduced by approximately 27 percent through helical swirl-induced chamber mixing, directly addressing operator toxic exposure risk in open-cabin V212 tractor operation.
- Brake thermal efficiency gain of 4.8 percent at 80 percent rated load, equivalent to approximately 13 litres of diesel fuel saved per tractor per working season.
- Manufacturing cost of Rs. 2,800 per unit — 18 percent below OEM replacement — using standard laser cutting, CNC perforation, roll forming, and TIG welding achievable in a rural fabrication workshop.
- 13.2 Future Research Directions
- Engine dynamometer validation: V212 test bed at 1800 to 2600 rpm and 40 to 100 percent load; backpressure, acoustic power, and emission measurements.
- Impedance tube acoustic testing per ISO 10534-2: transmission loss from 200 to 4000 Hz.
- LES simulation: capturing pulsating exhaust at 36.7 Hz and cyclic acoustic-turbulence interaction.
- DPF integration: backpressure-compatible particulate filter design for BS-VI/TREM-IV compliance paired with the nozzle muffler.
- Field CO measurement: operator-position concentration monitoring during tillage and headland turning under representative wind conditions.
- Multi-engine scale-up: scaled insert fabrication and testing for 35 to 50 HP range (Mahindra 575 DI, Eicher 380) and heavy truck platforms (Ashok Leyland U-3718).

Acknowledgements

The authors sincerely thank their project guide from the Department of Aerospace Engineering for reviewing this work multiple times with patience and technical honesty — each review made the project stronger than the last. This team began with no prior experience in CFD simulation or internal flow design and built every concept from scratch; that journey would not have been possible without the

International Research Journal on Advanced Engineering Hub (IRJAEH)
e ISSN: 2584-2137
Vol. 04 Issue: 03 March 2026
Page No: 1587-1602
https://irjaeh.com
https://doi.org/10.47392/IRJAEH.2026.0211

institutional support, library resources, and reference materials provided by Mahendra Engineering College (Autonomous), Namakkal. We also acknowledge the Head of the Department, the faculty who reviewed our presentations, and the department staff whose quiet, consistent support kept this work on track.

References

[1]. P. Huang et al., "Acoustic attenuation performance and optimization of split-stream rushing exhaust mufflers," Applied Sciences, vol. 15, art. 4722, 2025.
[2]. Y. Zhang et al., "Design and optimization of exhaust muffler for L24 diesel engine," Noise Control Engineering Journal, vol. 73, no. 1, pp. 77–94, 2025.
[3]. Z. Liu et al., "Duct metamaterial muffler with composite acoustic porous media: acoustic optimization," Materials, vol. 18, art. 4873, 2025.
[4]. M. Yimer and R. B. Nallamothu, "Reduction of the noise from the engine, modification of reactive muffler and performance analysis," Discover Applied Sciences, vol. 7, art. 849, 2025.
[5]. H. Kepekçi and M. E. Ağca, "Numerical investigation of the thermal and acoustic effect of material variations on the exhaust muffler," International Journal of Automotive Engineering and Technologies, vol. 13, no. 1, pp. 33–44, 2024.
[6]. F. Li et al., "Structural performance analysis and optimization of small diesel engine exhaust muffler," Processes, vol. 12, art. 2186, 2024.
[7]. S. D. Kumar, "Design and analysis of a muffler for engine exhaust noise and heat reduction," SAE Technical Paper 2021-28-0128, 2021.
[8]. Development of muffler design and its validation," Applied Acoustics, vol. 180, 108132, 2021
[9]. E. Jang and C. Doe, "Methods for evaluating in-duct noise attenuation performance in a muffler design problem," Journal of Sound and Vibration, vol. 464, 114982, 2020.
[10]. Erkan Dokumaci, Duct Acoustics Fundamentals and Applications to Mufflers and Silencers, Cambridge University Press, 2020.
[11]. M. L. Munjal and K. M. Kumar, "Direct estimation and experimental validation of acoustic source characteristics of diesel exhaust systems," Applied Acoustics, 2019.
[12]. R. B. K., "A review on current techniques for acoustic performance of automobile exhaust muffler," International Journal of Engineering Research & Technology (IJERT), 2018.
[13]. M. A. H. Habib et al., "3D CFD based optimization technique for muffler design of a motorcycle," Applied Mechanics and Materials, vol. 860, pp. 52–57, 2016.
[14]. M. Dixit, V. Sundaram, and S. Kumar, "Optimization of muffler acoustics performance using DFSS approach," SAE Technical Paper 2016-01-1292, SAE International, 2016.
[15]. Manohar L. Munjal, Acoustics of Ducts and Mufflers with Application to Exhaust Design, 2nd ed., Wiley, 2014
[16]. CFD research on aerodynamic performance of complicated resistance muffler," Applied Mechanics and Materials, vol. 34-35, pp. 1274–1278, 2013.